Research Article

Journal of MASS SPECTROMETRY

Received: 17 May 2008 Accepted: 12 August 2008 Published online in Wiley Interscience: 14 October 2008

(www.interscience.com) DOI 10.1002/jms.1502

Diagnostic fragment-ion-based extension strategy for rapid screening and identification of serial components of homologous families contained in traditional Chinese medicine prescription using high-resolution LC-ESI-IT-TOF/MS: *Shengmai injection* as an example

Chaonan Zheng,[a†] Haiping Hao,[a†] Xuan Wang,[a] Xiaolan Wu,[a] Guangji Wang,[a*] Guowei Sang,[b*] Yan Liang,[a] Lin Xie,[a] Chunhua Xia[a] and Xilin Yao[a]

The paper presents a modified and universally applicable diagnostic fragment-ion-based extension strategy (DFIBES) to efficiently process the information acquired by liquid chromatography-electrospray ionization source in combination with hybrid ion trap and high-resolution time-of-flight mass spectrometry [LC-(ESI)-IT-TOF/MS], facilitating the structural determination of serial components contained in traditional Chinese medicine prescription (TCMP). The key advantage of DFIBES is that it facilitates the rapid classification of the complicated peaks into well-known chemical families, which significantly simplifies the complicated procedures of structural characterization. Moreover, considering that a certain family of compounds usually produces identical fragment ions, the DFIBES would be widely applicable to many other families of compounds identification besides the presently validated ginsenosides and lignans. *Shengmai injection*, composed of *Panax ginseng, Radix ophiopogonis*, and *Schisandra chinensis*, was taken as a TCMP example to conduct and validate the proposed DFIBES. Diagnostic fragment ions (DFI) for each chemical family contained in *Shengmai injection* was firstly determined or proposed from the separated analysis of 15 authentic standards and the extract of *S. chinensis*. The ESI-MS^n fragmentation patterns of ginsenosides and lignans were then systematically studied for developing the 'structure extension' approach. Upon LC-IT-TOF/MS analysis and DFIBES, more than 30 ginsenosides and 20 lignans have been rapidly detected and identified from *Shengmai injection*, supporting that the DFIBES is a very powerful strategy and would be widely applicable for the complicated components identification from TCMP and other complicated mixtures.

Keywords: LC-IT-TOF/MS; serial components; diagnostic fragment-ion-based extension strategy (DFIBES); structure characterization; traditional Chinese medicine prescription (TCMP); *Shengmai injection*

Introduction

Traditional Chinese medicine prescription (TCMP), a formula of several single herbs combined at an intrinsic mass ratio,[1] is the main form of applying traditional Chinese medical science for clinical treatment. Although many TCMPs have been clinically applied for thousands of years and their pharmacological activities have been confirmed in abundant modern scientific studies, it remains largely a secret that which and how active constituents produce the effectiveness, which has now become a main bottleneck restricting the TCMP modernizations. Unambiguously, detection and identification of the active components in TCMP are the prerequisite step and a key to disclose the secret. Therefore, elucidating components contained in TCMP is urgently necessary and of great significance for revealing the scientific bases and rationality of prescription compatibility and pharmacological mechanisms, optimizing the preparation technology, establishing standards for quality control as well as realizing the modernization of traditional Chinese medicine. However, it is still a great challenge to the global detection and structural characterization of complicated components contained in TCMP, despite the recent great advance in the analytical tools and methods.

* *Correspondence to: Guangji Wang, Key Lab of Drug Metabolism & Pharmacokinetics, China Pharmaceutical University, Nanjing 210038, China. E-mail: guangjiwang@hotmail.com*

** *Guowei Sang, National Institute for the Control of Pharmaceutical and Biological Products, Beijing 100050, China. E-mail: sanggw@nicpbp.org.cn*

† *These authors contributed equally to this work.*

a *Key Lab of Drug Metabolism & Pharmacokinetics, China Pharmaceutical University, Nanjing 210038, China*

b *National Institute for the Control of Pharmaceutical and Biological Products, Beijing 100050, China*

Journal of MASS SPECTROMETRY

In the past few years, reports on the detection and identification of active ingredients in TCMP have been steadily increasing, especially for the recently accelerated development of various hyphenated and hybrid mass spectrometry (MS) techniques such as liquid chromatography/mass spectrometry (LC/MS),[2–4] tandem mass spectrometry (MS/MS),[5–9] LC/ion trap (II)/MS,[10–15] triple quadrupole linear ion trap mass spectrometry (QTRAP),[16,17] LC/time-of-flight (TOF)/MS,[18–21] and quadrupole time-of-flight mass spectrometry (QqTOF-MS/MS).[22–24] Undoubtedly, the combined use of TOF/MS with various tandem mass spectrometry would be a better choice for identifying the complicated components contained in TCMP, in the view of that they provide both elemental compositions and the multiple-stage of fragmentation patterns information. A good example was rapid separation and identification of phenolic and diterpenoid constituents from Radix Salvia miltiorrhizae by sequential HPLC-diode array detection (DAD), HPLC/ESI-TOF-MS, and HPLC/ESI-MS^n analysis reported by Zhu *et al*.[20] In another study, Li *et al*.[22] successfully analyzed steroid saponins from the rhizomes of *Dioscorea panthaica* using ESI-QqTOF-MS/MS and atmospheric pressure chemical ionization (APCI)-IT-MS/MS. However, it can be imaged that the combined application of tandem mass spectrometry and TOF/MS to identifying complicated components in TCMP would generate a large quantity of information content which, despite very helpful for the structural elucidation, will lead to a new challenge of information processing. One component can give rise to several quasi-molecular ions, and each quasi-molecular ion can produce a series of fragment ions in Collision induced dissociation (CID) mode. Moreover, TCMP contains hundreds of components and the complex matrix interferences are very comprehensive. These all make it a rather difficult and tedious task to dealing with the extremely large data set of fragmentation information. Therefore, a strategy for efficient mass spectra analysis is highly demanded for rapid characterization of the naturally occurring substances in TCMP. To date, very few strategies involved have been published, despite the growing number of reports using mass spectrometry for components characterization in recent years.[2–24] Qu *et al*.[25] recently described an energy gradient neutral loss scan (EGNLS) strategy for this purpose. Although this strategy was efficient for rapid identification of glycosides, it cannot be extended to other kinds of components.

This study was thus designed to develop a universal strategy, diagnostic fragment-ion-based extension strategy (DFIBES), for rapid components identification from TCMP based on the use of the liquid chromatography-electrospray ionization source in combination with hybrid ion trap and high-resolution time-of-flight mass spectrometry (LC-IT-TOF/MS), which integrates the capabilities of IT and TOF/MS along with LC for separation in a single instrument. DFIBES was originally proposed from the known fact that the components contained in TCMP could usually be structurally classified into several families and a same family of components usually contained same carbon skeleton or substructures, from which the same fragment ions (diagnostic ions) can be produced from the tandem mass spectrometry. In order to examine the feasibility, reliability, and universality of the present approach, *Shengmai injection*, derived from *Sheng Mai San*, was set as a TCMP example. *Shengmai injection (or San)*, comprised of three known herbs, namely *Panax ginseng*, *Radix ophiopogonis*, and *Schisandra chinensis baill*, has long been playing important roles in the treatment of coronary atherosclerotic cardiopathy and viral myocarditis, and it is also capable of raising tumor patients' immunity.[26,27] However, little is known about its effective constituents. On the basis of the previous research on the individual botanicals, ginsenoside,[27,28] ophiopogonin,[29,30] ophiopogonone,[31,32] and lignan[2,33] have been proposed as the active components in *P. ginseng, R. ophiopogonis, and S. chinensis*, respectively. Using the presently established methodology, more than 30 ginsenosides and 20 lignans, was originally identified from *Shengmai injection*.

Experimental

Chemicals and reagents

Authentic standards of 20(S)-ginsenoside R1, Rb1, Rb2, Rb3, Rc, Rd, Re, Rg1, Rg2, Rg3, Rh1, and Rh2 were purchased from Department of Nature Medical Chemistry in Jilin University (Jilin, China), and Schizandrin A, Schizandrin B, Schizandrol A, and the extract of *S. chinensis* were from National Institute for the Control of Pharmaceutical and Biological Products (Beijing, China). *Shengmai injection* was obtained from SZYY Group Pharmaceutical Limited (Jiangsu, China). HPLC-grade acetonitrile was from Tedia Inc. (Fairfield, OH). Deionized water was purified using a Milli-Q system (Millipore, Milford, MA, USA). Glacial acetic acid, *n*-butanol, and other chemicals and solvents were all of analytical grade.

Sample preparation

A volume of 40 µl of *Shengmai injection* was diluted 10-fold with water in an Eppendorf tube, followed by 30 s of vortexing using a vortex mixer (Scientific industries, Inc., USA). Then, analytes were extracted from the injection using a single step of liquid–liquid extraction. For this, 2 ml of water saturated *n*-butanol (five volumes) was added to each tube and mixed by vortexing for 3 min. The well-vortexed solution was then centrifuged at 5000 g for 10 min and 1.6 ml of the upper organic layer was transferred to a new Eppendorf tube and evaporated to dryness with nitrogen. The residues were then reconstituted in 500 µl methanol followed by centrifugation at 20 000 g for 10 min. A volume of 5 µl supernatant was injected into the LC-IT-TOF/MS for analysis.

Instrumentation and conditions

LC experiments were conducted using a Shimadzu (Kyoto, Japan) HPLC system consisting of an LC-20AB binary pump, an SIL-20AC autosampler, a CTO-20AC column oven, and an SPD-M20A PDA. Chromatographic separation of analytes was achieved using a 250 × 4.6 mm^2 Hypersil ODS2 C18 analytical column (Dalian, China). The column and autosampler tray temperatures were set at 35 and 4 °C, respectively. The mass detection was carried out using a Shimadzu ion trap/time-of-flight hybrid mass spectrometry (IT-TOF/MS) (Shimadzu, Kyoto, Japan), equipped with an electrospray ionization source. In automatic mode, all ions were firstly accumulated in octopole and then rapidly pulsed into IT for MS^n analyses according to the criteria settings. All ions produced were finally introduced into the TOF instrument for accurate mass determinations. Data acquisition and analysis was performed with LC Solution 3.0 software (Shimadzu, Kyoto, Japan).

Conditions for ginsenoside, ophiopogonin, and ophiopogonone

A mobile phase composed of eluent A (0.02% acetic acid in water, v/v) and B (0.02% acetic acid in acetonitrile, v/v) with a gradient elution was employed for the separation. The mobile phase was consecutively programmed as follows: an isocratic elution of 20% B for the first 15 min, followed by a linear gradient elution of 20–35% B from 15 to 35 min, 35–40% B from 35 to 55 min, and 40–65% B from 55 to 70 min. After holding the solvent composition of 65% B for the next 5 min, the column was returned to its starting conditions. The flow-rate was 1 ml/min with a post-column splitting into two flows, one for UV detection and the other for MS detection.

The optimized MS conditions were as follows: negative ion mode; electrospray voltage, −3.5 kV; CDL temperature, 200 °C; block heater temperature, 200 °C; nebulizing gas (N_2), 1.5 l/min; drying gas (N_2) pressure, 0.1 MPa. Mass spectra were acquired in the range of *m/z* 200–1500 for MS^1, 100–1500 for MS^2, and 50–1500 for MS^3. The MS^n data were collected in an automatic mode and the software could automatically select precursor ions for MS^n analysis according to criteria settings (such as ion intensity). Argon was used as the collision gas and the collision energy was set at 50% both for MS^2 and MS^3. Prior to data acquisition, the instrument was calibrated with sodium TFA clusters against the entire mass range (*m/z* 50–5000) specified for the instrument.

Conditions for lignan

The chromatographic conditions for lignan were the same as those used for ginsenoside except for the composition of the mobile phase (without acetic acid). The mass spectrometer was operated in positive ion mode for lignan analysis with electrospray voltage at 4.5 kV. Mass spectra were acquired in the range of *m/z* 300–600 for MS^1, 100–600 for MS^2, and 50–600 for MS^3. Other parameters were all the same as those described for ginsenosides.

Diagnostic fragment-ion-based extension strategy (DFIBES)

To facilitate the mass spectra analysis for structure characterization, we proposed a modified strategy, DFIBES, from the previously reported ones[22,34] based on the following evidence. TCMP components can be structurally sorted into several classes based on their carbon skeletons. It is therefore acceptable and easily understood that the compounds with the same carbon skeleton (a serial components or one chemical 'family') are subjected to the similar fragmentation pathway in CID mode and thus generating a common diagnostic ion from the common carbon skeleton. Therefore, the diagnostic ion can be used firstly for rapidly selecting out the peaks as the components of a certain chemical family. A further 'structure extension' approach, similar to 'formula extension' approach proposed by Kujawinski and Behn,[35] can then be applied to the detailed structure characterizations for the components detected.

The critical, first step of DFIBES is to find the diagnostic fragment ions (DFI) for each chemical family. For this purpose, 15 representative authentic standards were separately infused to IT-TOF/MS to determine the common DFI. The standard extract of *S. chinensis* containing various lignan components was also used for determining as many as possible of the lignan families, considering that it was very difficult to obtain the authentic standards of lignan type components. Once the carbon skeleton being determined by the recognition of DFI, the chemical groups of a certain compound can easily be deduced from the accurate mass distances between quasi-molecular ions and the corresponding serial fragment ions.

Results and Discussion

Establishment and optimization of the DFIBES strategy

DFI determinations and fragmentation pattern analysis for ginsenosides

Ginsenosides can be roughly classified into three types: protopanaxadiol, protopanaxatriol, and oleanolic acid-type ginsenoside, based on the structures of the aglycones. On the basis of structures of the branched chain at C-20, ginsenosides are subdivided into A, B, C, D, and E, five types (Fig. 1) in this study. The preliminary analysis with reference compounds confirmed that negative ion mode was more sensitive, and provided straightforward structural information of ginsenosides as compared with that by positive ion mode, which was in agreement with those previously reported.[36,37] Consequently, negative ion mode was operated to investigate the DFI and the fragmentation patterns of ginsenosides with 12 glycoside standards (shown in Fig. 1, representing two common types: protopanaxadiol and protopanaxatriol).

The DFI was firstly determined from the fragment ions of ginsenoside standards (Table 1). For type A ginsenosides, the DFI were determined as *m/z* 459.3844($C_{30}H_{51}O_3^-$) corresponding to [aglycone − H]$^-$ (DFI 1) and 783.4901 ($C_{42}H_{71}O_{13}^-$) corresponding to [aglycone + $2C_6H_{10}O_5$-H]$^-$ (DFI 2). Ions at *m/z* 475.3793($C_{30}H_{51}O_4^-$) corresponding to [aglycone − H]$^-$ (DFI 1) and *m/z* 391.2854($C_{24}H_{39}O_4^-$) corresponding to [aglycone − C_6H_{12}-H]$^-$ (DFI 2) were determined as the DFI for type B ginsenosides. Similarly, the DFI for type C, D, and E ginsenosides were proposed as [aglycone−H]$^-$ ions: 441.3738($C_{30}H_{49}O_2^-$) for C, D type protopanaxadiol, 457.3687 ($C_{30}H_{49}O_3^-$) for C, D type protopanaxatriol, and 455.3531($C_{30}H_{47}O_3^-$) for type E (oleanolic acid-type) from their respective fragmentation patterns (Fig. 2), which were proposed based on comparing the structure similarities with type A and B ginsenosides and also by referencing to the previous reports. The structures of DFI for each class of ginsenosides are shown in Fig. 2.

To develop the 'structure extension' strategy, the fragmentation pattern of each subfamily of ginsenosides was analyzed in detail. The ESI-MS spectra exhibited that ginsenosides produced various singly and doubly charged quasi-molecular ions including [M−H]$^-$ and [M − 2H]$^{2-}$ as well as adduct ions [M + AcO]$^-$, [M + 2AcO]$^{2-}$, and [M + AcO-H]$^{2-}$, formed from mobile phase additive acetic acid. These observed pseudomolecular ions were very useful for determining the molecular weights of the detected ginsenosides. Only the [M − H]$^-$ ions and their corresponding fragment ions were provided in detail in Table 1, in the view of that other pseudomolecular ions produced much fewer useful fragment ions.

The fragmentation patterns of each subfamily of ginsenosides are summarized in Fig. 2 by selecting one representative compound. The nomenclature proposed by Domon and Costello[38] with some adaptation was adopted to denote the fragment ions. The ions containing the charge at the reducing terminus were termed Y-type ions, whereas those ions retaining the charge on the carbohydrate residue were designated as B-type ions. The oligosaccharide chains at C-20 were defined as α-chain because the glycosidic bond cleavage preferentially occurred at this position, whereas those at C-3 or C-6 were defined as β-chain.

Journal of MASS SPECTROMETRY

Protopanaxadiol			
Type	Ginsenoside	R_1	R_2
A	Ra1	-Glc^2-Glc	-Glc^6-Arap^4-Xyl
A	Ra2	-Glc^2-Glc	-Glc^6-Araf^4-Xyl
A	Ra3	-Glc^2-Glc	-Glc^6-Glc^3-Xyl
A	Rb1^S	-Glc^2-Glc	-Glc^6-Glc
A	Acetyl-Rb1	-Glc^2-Glc^6-Ac	-Glc^6-Glc
A	Rb2^S	-Glc^2-Glc	-Glc^6-Arap
A	Rb3^S	-Glc^2-Glc	-Glc^6-Xyl
A	Rc^S	-Glc^2-Glc	-Glc^6-Araf
A	Rd^S	-Glc^2-Glc	-Glc
A	Rs1	-Glc^2-Glc^6-Ac	-Glc^6-Arap
A	Rs2	-Glc^2-Glc^6-Ac	-Glc^6-Araf
A	Rs3	-Glc^2-Glc^6-Ac	-H
A	20 (*S*)-Rg3^S /20(R)-Rg3	-Glc^2-Glc	-H
A	20 (*S*)-Rh2^S /20(R)-Rh2	-Glc	-H
A	Notoginsenoside-R4	-Glc^2-Glc	-Glc^2-Glc^6-Xyl
A	F2	-Glc	-Glc
C	Rg5	-Glc^2-Glc	-H
D	Rk1	-Glc^2-Glc	-H
Protopanaxatrial			
Type	Ginsenoside	R_1	R_2
B	Re^S	-Glc^2-Rha	-Glc
B	Rf	-Glc^2-Glc	-H
B	Rg1^S	-Glc	-Glc
B	20 (*S*)-Rg2^S /20(R)-Rg2	-Glc^2-Rha	-H
B	20 (*S*)-Rh1^S /20(R)-Rh1	-Glc	-H
B	F1	-H	-Glc
B	Notoginsenoside-R1^S	-Glc^2-Xyl	-Glc
B	Notoginsenoside-R2	-Glc^2-Xyl	-H
C	Rh4	-H	-O-Glc
C	F4	-H	-O-Glc^2-Rha
D	Rk3	-H	-O-Glc
D	Rg6	-H	-O-Glc^2-Rha
Oleanolic acid			
Type	Ginsenoside	R_1	R_2
E	Ro	-	-

Glc = β-D-glucose
Rha = α-L-rhamnose
Arap = α-L-arabinose (pyranose)
Araf = α-L-arabinose (furanose)
Xyl = β-D-xylose
GlcUA = β-D-glucuronide

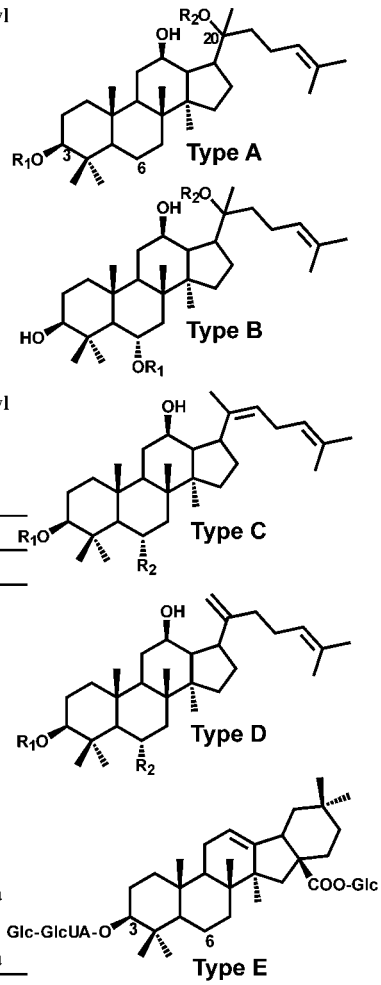

Figure 1. Structures of ginsenosides. ^{S}Constituents with standards.

Fragment ions yielded by the cleavage of top-right aliphatic chain or the neutral loss of H_2O were designated as E-type ions.

We took ginsenoside Rc (type A) as an example to describe the fragmentation patterns of ginsenosides in detail. The $[M-H]^-$ ion (*m/z* 1077.59) produced fragment ions at *m/z* 945.5443, 915.5336, 783.4888, 765.4773, 621.4359, 537.3427, 459.3835, and 375.2910 in MS^2 through the $Y_{1\alpha}$, $Y_{1\beta}$, $Y_{0\alpha}$ or $[Y_{1\alpha} - B_{1\beta}]$, E_1, $[Y_{0\alpha} - B_{1\beta}]$ or $[Y_{0\beta} - B_{1\alpha}]$, $[Y_{0\alpha} - B_{1\beta} - E_2]$, $[Y_{0\alpha} - B_{2\beta}]$, and $[Y_{0\alpha} - B_{2\beta} - E_2]$ fragmentations respectively (Fig. 2). The mass differences between the parent ion (*m/z* 1077.5856) and the fragment ions *m/z* 945.5443 and 915.5336 were 132.0413 and 162.0520 Da, indicating the loss of a pentose residue and a hexose residue, respectively. The intensity of ion at *m/z* 945.5443 from losing a pentose residue at C-20 was much greater than that of ion at *m/z* 915.5336 from losing a hexose residue at C-3. Similar results were also observed for most other ginsenosides, indicating that the cleavage of the oligosaccharide residue preferentially happened at C-20, which was consistent with the previous results reported by Liu *et al*.[37] The fragment ion at *m/z* 783.4888 could be theoretically produced from the loss of a disaccharide at C-20 ($B_{2\alpha}$) or the combined loss of two terminal residues ($B_{1\alpha} + B_{1\beta}$) at C-20 and C-3. However, we considered that the former fragmentation pathway should be the major one since its further neutral loss of H_2O to form E_1 (*m/z* 765.4773) was observed. Similarly, the fragment ion at *m/z* 621.4359 could be attributed to $[Y_{0\alpha} - B_{1\beta}]$ or $[Y_{0\beta} - B_{1\alpha}]$ fragmentations, while the former was the major pathway as

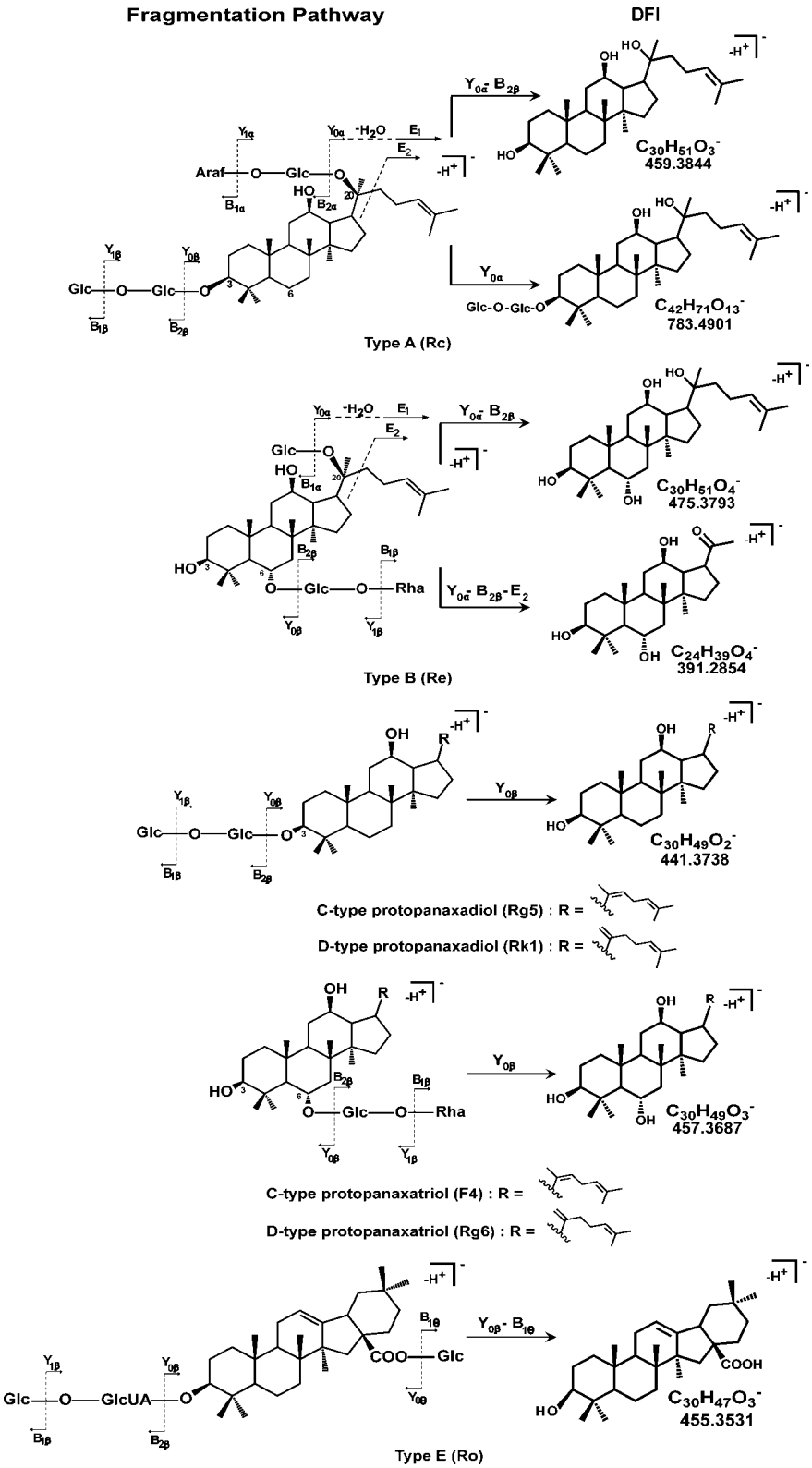

Figure 2. The proposed fragmentation pathways and the structures of diagnostic fragment ions (DFI) for each type of ginsenosides.

evidenced by its further neutral loss of C_6H_{12} to form $[Y_{0\alpha} - B_{1\beta} - E_2]$ (*m/z* 537.3427). Moreover, previous reports also supported that the glycosidic bonds were more stable at C-3 position than C-20 position.[39] The ion at *m/z* 459.3835 was produced from the loss of all sugar units from $[M - H]^-$ ion to form [aglycon − H]$^-$ ion ($[Y_{0\alpha} - B_{2\beta}]$,) which further produced the [aglycone − H − C_6H_{12}]$^-$ ion ($[Y_{0\alpha} - B_{2\beta} - E_2]$, *m/z* 375.2910) by losing the side chain. The selected MS^3 analysis of the ions at *m/z* 945.54, 783.48, 621.43,

Journal of MASS SPECTROMETRY

Table 1. LC-ESI-MS and MS^n ions of ginsenoside standards

Ginsenoside	Pseudomolecular ions (PI) $[M-H]^-$ *m/z* (% base peak, ppm[a])	Fragment ions (MS^2) *m/z* (% base peak)	Fragment ions (MS^3) *m/z* (% base peak)
Rh2	621.4352 (5.5, −3)	537.3418(3.0), **459.3790(100)***, 375.2885(38.3)	375.2871(100).
Rb1	1107.5990 (13.9, 3)	945.5455(58.7), **783.4893(66.8)***, 621.4360(55.9), 603.4229(0.2), 537.3449(7.8), 459.3848(57.5)*, 375.2908(40.1)	459.3877(99.7)*.
Rc	1077.5880 (12.3, 3)	**945.5443(42.5)**, 915.5336(8.44), **783.4888(100)***, 765.4773(12.5), **621.4359(83.1)**, 537.3427(9.6), **459.3835(76.3)***, 375.2910(37.3)	783.4879(100)*; 621.4312(20.2), 537.3406(16.38), 459.3844(100)*, 375.2907(16.4); 459.3769(29.5)*, 375.2867(100); 375.2890(100).
Rb2	1077.5870 (24.8, 2)	**945.5437(50.4)**, **783.4885(100)***, 765.4736(8.3), **621.4356(69.6)**, 603.4221(3.3), 537.342(9.5), **459.3831(69.5)***, 441.3771(0.2), 375.2905(38.8)	783.4975(100)*, 459.3854(76.23)*; 459.3769(100)*; 375.2970(100); 375.2883(100).
Rb3	1077.5850 (28.2, 0)	**945.5440(39.5)**, **783.4881(100)***, 765.4774(9.3), **621.4361(83.7)**, 603.4241(3.5), 537.3432(12.4), **459.3839(81.2)***, 375.2911(42.3)	459.3769(100)*; 537.3445(), 375.2852(100); 459.3862(100)*; 375.2914(100).
Rd	945.5468 (100, 4)	**783.4876(100)***, **621.4355(55.2)**, 537.3417(16.4), **459.3831(76.9)***, 441.3722(1.4), 375.2909(55.7)	459.3822(100)*, 375.2907(66.4); 537.3380(18.34), 459.3878(34.03)*, 375.2898(100); 375.2927(100).
Rg3	783.4881 (100, −2)	**621.4343(62.3)**, **537.3386(19.7)**, **459.3801(88.5)***, 375.2883(100)	459.3787(100)*, 375.2911(63.6); 375.2961(100); 375.2891(100).
Notoginsenoside R1	931.5311 (100, 4)	799.4847(16.0), **637.4320(31.1)**, **475.3796(100)***, 457.3682(3.2), 391.2865(54.2)*	475.3782(100)*, 391.2851(51.2)*; 391.2847(100)*.
Rg1	799.4880 (44.4, 4)	**637.4353(84.3)**, **475.3805(100)***, 391.2870(35.6)*	475.3784(100)*, 391.2918(60.85)*; 391.2860(100)*.
Re	945.5454 (90.9, 3)	799.4839(7.6), **783.4888(10.9)**, **637.4324(24.3)**, 619.4207(12.5), **475.3796(100)***, 457.3691(3.5), 391.2865(56.2)*	619.4223(81.0), 391.2851(100)*; 475.3806(45.87)*, 391.2907(100)*; 391.2842(100)*.
Rg2	783.4894 (100, −0.8)	**637.4267(14.6)**, 619.4142(7.7), **475.3741(100)***, 457.3628(1.9), 391.2818(91.0)*	475.3734(100)*, 391.2799(45.9)*; 391.2824(100)*.
Rh1	637.4293 (50.9, −4)	**475.3749(100)***, 391.2850(56.0)*	391.2799(100)*.

[a] : differences between the observed and theoretical values; * : the detected DFI. The fragment ions with high response (intensity > 10 000) generated in MS^2 which were shown in bold font and underlined were automatically selected for MS^3 fragmentations.

459.38 further supported the proposed fragmentation patterns of ginsenoside Rc. In summary, glycosidic bond cleavage (Y, B) and neutral loss of H_2O (E_1) or top-right aliphatic chain (E_2) were the three major fragmentation pathways for ginsenoside Rc and also for other ginsenosides.

DFI determinations and fragmentation pattern analysis for lignan

The lignans, composed of A, B, and C rings, could be structurally classified into five subfamilies (Fig. 3) according to the substituents of different types on the three rings as follows: no oxygen group on C ring (I), a hydroxy group at C-6 or C-7 on C ring (II), a hydroxy group at C-7 on C ring and a substituent of phenolic ester on aromatic ring (III); a hydroxy group at C-7 and a esterfunction group at C-6 on C ring (IV); a lactone in eleven-member ring (V). The classification was also supported by their fragmentation behaviors. The positive scan mode gave $[M+H]^+$ or $[M+Na]^+$ as pseudomolecular ions for lignans, while there was no signal detected in the negative ion scan mode. On the basis of the present mass analysis of lignan standards (Table 2) and the total lignans extract of *S. chinensis*, combined with previous literature reports,[11,40,41] we proposed DFI and fragmentation pathways for the five types of lignans as follows and summarized in Fig. 4.

Type I: The predominant fragment ion of $[M+H]^+$ was $[M-CH_3O\cdot-C_5H_{10}+H]^{+\cdot}$ ($[E_1-E_2]$), produced by losing firstly a $CH_3O\cdot$ radical, and then undergoing the sequential cleavages of C6–7 and C9–10 bonds, the loss of C_5H_{10} and the eight-member ring transformation to five-member ring. The fragmentation of $[M+Na]^+$ was featured with the combined elimination of methyl and methoxyl radicals, which lead to the formation of $[M-CH_3\cdot-CH_3O\cdot+Na]^+$ (E). According to the previous reports,[11,41,42] the elimination of methyl ($CH_3\cdot$, 15.0235) or methoxyl (CH_3O, 31.0184) radical, observed from this type, could be explained by the presence of several methoxyl groups connected to A and B rings. Both of $[M-CH_3O\cdot-C_5H_{10}+H]^{+\cdot}$ and $[M-CH_3\cdot-CH_3O\cdot+Na]^+$ ions can be used as DFI.

(Type I)	R_1	R_2	R_3	R_4	R_5	R_6
Schizandrin A[S]	$-CH_3$	$-CH_3$	$-CH_3$	$-CH_3$	$-CH_3$	$-CH_3$
Schizandrin B[S]	$-CH_3$	$-CH_3$	$-CH_3$	$-CH_3$	$-CH_2-$	
γ-Schizandrin	$-CH_2-$		$-CH_3$	$-CH_3$	$-CH_3$	$-CH_3$
Schisanhenol	$-CH_3$	$-CH_3$	$-CH_3$	-H	$-CH_3$	$-CH_3$
Gomisin L1	$-CH_3$	$-CH_3$	-H	$-CH_3$	$-CH_2-$	
Gomisin L2	-H	$-CH_3$	$-CH_3$	$-CH_3$	$-CH_2-$	
Gomisin K1	-H	$-CH_3$	$-CH_3$	$-CH_3$	$-CH_3$	$-CH_3$
Gomisin K2	-H	$-CH_3$	$-CH_3$	$-CH_3$	$-CH_3$	$-CH_3$
Gomisin N	$-CH_3$	$-CH_3$	$-CH_3$	$-CH_3$	$-CH_2-$	
(Type II)	R_1	R_2	R_3	R_4	R_5	R_6
Isoschizandrin	$-CH_3$	$-CH_3$	-H	-H	-OH	$-CH_3$
Schizandrol A[S]	$-CH_3$	$-CH_3$	-H	-H	$-CH_3$	-OH
Schizandrol B	$-CH_2-$		-H	-H	$-CH_3$	-OH
Gomisin O	$-CH_2-$		-H	-OH	$-CH_3$	-H
Epigomisin O	$-CH_2-$		-OH	-H	$-CH_3$	-H
Gomisin S	$-CH_3$	$-CH_3$	-OH	-H	$-CH_3$	-H
(Type III)	R_1	R_2	R_3			
Angeloyl gomisin H	-OAng	$-CH_3$	-OH			
Tigloyl gomisin H	-OTig	$-CH_3$	-OH			
(Type IV)	R_1	R_2	R_3	R_4	R_5	
Schisantherin A	$-CH_3$	$-CH_3$	$-CH_2-$		-Obz	
Schisantherin B	$-CH_3$	$-CH_3$	$-CH_2-$		-OAng	
Schisantherin C	$-CH_3$	$-CH_3$	$-CH_2-$		-OTig	
Gomisin F	$-CH_2-$		$-CH_3$	$-CH_3$	-OAng	
Gomisin G	$-CH_2-$		$-CH_3$	$-CH_3$	-OBz	
Angeloyl gomisin Q	$-CH_3$	$-CH_3$	$-CH_3$	$-CH_3$	-OAng	
Tigloyl gomisin Q	$-CH_3$	$-CH_3$	$-CH_3$	$-CH_3$	-OTig	
(Type V)	R_1	R_2				
Gomisin D	-OH	$-CH_3$				

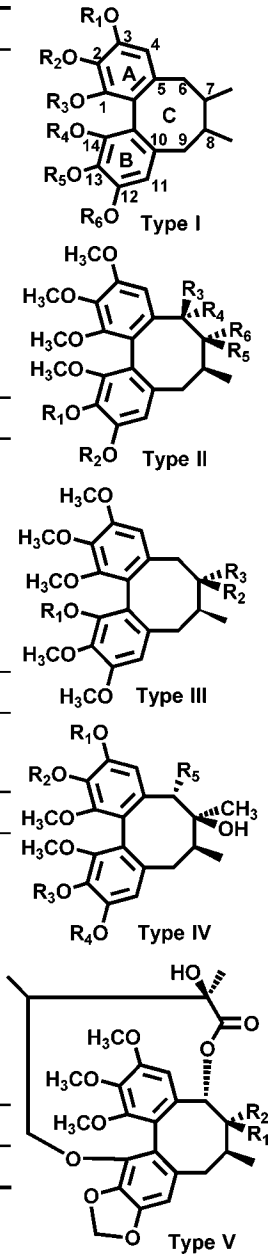

Figure 3. Structures of lignans. [S]Constituents with standards.

Type II: For this type of lignans, $[M + Na]^+$ ion was more intensive than $[M + H]^+$ ion due to the substitution of hydroxy group at C-6 or C-7 on C ring. However, fragmentation of $[M + H]^+$ ion could give much more structural information. The $[M + H]^+$ ion lost a H_2O molecule to form the product ion $[M - H_2O + H]^+$ (E_1), then undertook further elimination of methyl or methoxyl radical similar as quasi-molecular ions of type I. The elimination of H_2O could be considered a characteristic fragmentation of this type, and $[M - H_2O + H]^+$ ion can be used as DFI for this type.

Type III: $[M + Na]^+$ ion had greater signal intensity than $[M + H]^+$ ion, consistent with type II. $[M + H]^+$ ion readily lost one molecule of H_2O at C ring and the olefine ketone (C_5H_6O, 82.0418 or C_7H_4O, 104.0262) associated with phenolic ester at A or B ring. Similar fragmentation patterns have been found in the EI mass spectra.[41] Consequently, we chose $[M-H_2O-C_5H_6O/C_7H_4O+H]^+$ ($[E_2 - E_1]$) ion as the DFI.

Type IV: $[M + Na]^+$ ions, as the only pseudomolecular ions, exhibited predominant dissociation of carboxylic acid ($C_5H_8O_2/C_7H_6O_2$) at C ring and produced the DFI $[M - C_5H_8O_2/C_7H_6O_2 + Na]^+$ (E) ion (*m/z* 437.1571 or *m/z* 453.1884).

Type V: Lignans of this type showed remarkable $[M + Na]^+$ ions. The presence of lactone appeared to trigger the cleavage of eleven-member ring as well as the combined neutral loss of a CO and a H_2O molecule, and then the loss of a $C_6H_{12}O_2$ moiety. We selected characteristic product ion $[M - (CO + H_2O) + Na]^+$ ($[E_1 - E_2]$) as DFI.

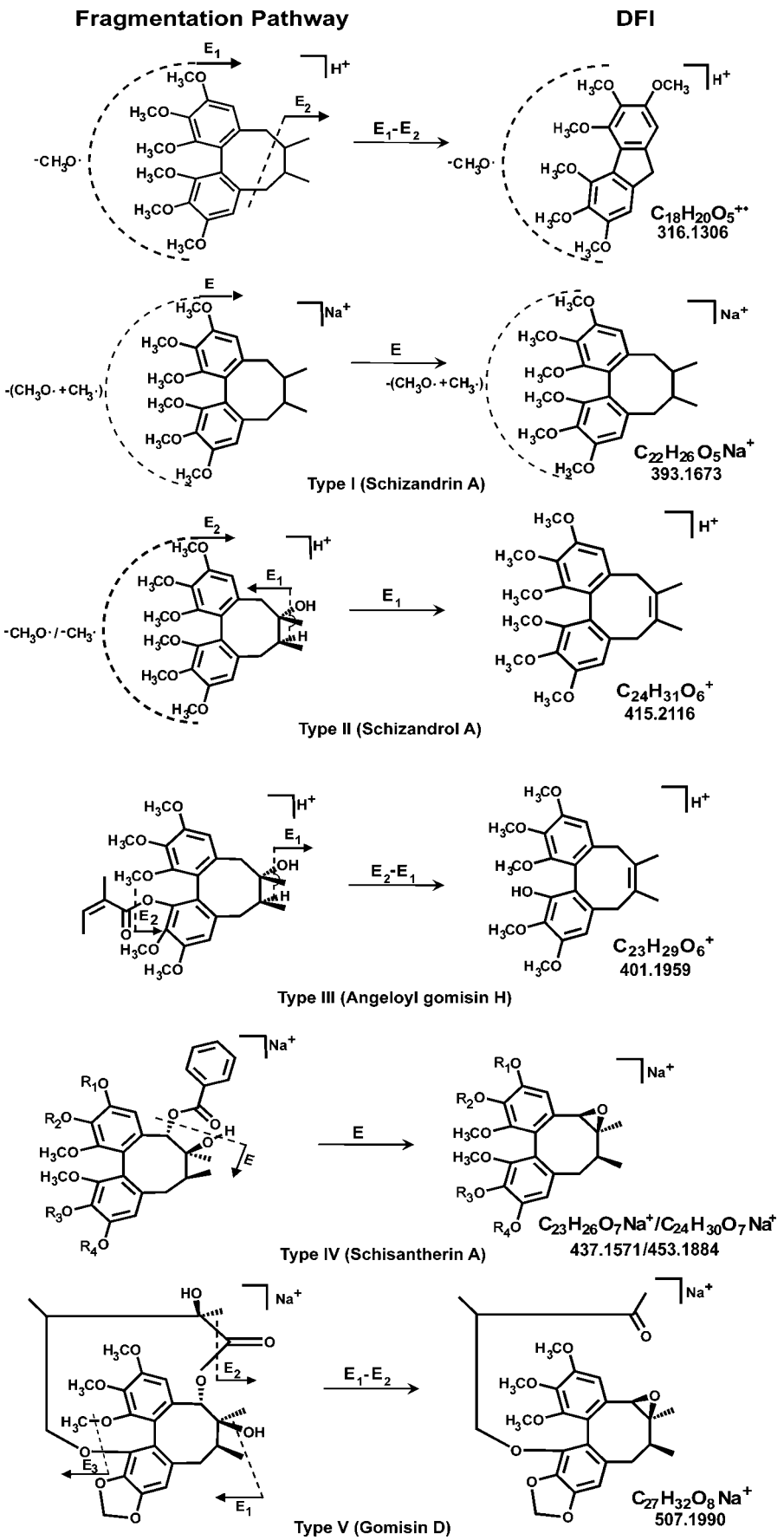

Figure 4. The proposed fragmentation pathways and the structures of diagnostic fragment ions (DFI) for each type of lignans.

Table 2. LC-ESI-MS and MS^n ions of lignan standards

Lignan	PI *m/z* (% base peak, ppm[a]) $[M+H]^+$	PI *m/z* (% base peak, ppm[a]) $[M+Na]^+$	Fragment ions (MS^2) *m/z* (% base peak)	Fragment ions (MS^3) *m/z* (% base peak)
Schizandrin A	417.2287 (100, 2)	439.2081 (60.79, −4)	MS^2 $[M+H]^+$: 402.2041(13.74), 386.2056(5.38), 371.1834(5.83), **347.1475(6.72)**, **332.1235(6.31)**, **316.1292(100)***, 301.1062(38.84), 285.1100(21.8); MS^2 $[M+Na]^+$: 393.1652(100)*.	317.1305(100), 316.1268(25.93)*, 301.1095(7.87); 302.1056(100), 301.1009(47.51); 301.1069(67.81), 285.1068(62.33), 270.0854(15.34), 242.0951(100), 227.0667(14.41).
Schizandrin B	401.1978 (100, 3)	423.1774 (76.79, −2)	MS^2 $[M+H]^+$: 386.1709(16.59), 370.1764(20.33), 355.1519(9.1), 331.1152(9.25), **300.0977(100)***, 285.0764(20.58), 269.0812(6.86), 242.0928(20.15), 227.0686(10.04); MS^2 $[M+Na]^+$: 377.1272(23.76)*.	286.0768(100), 285.0771(29.83), 269.0795(14.21), 227.0706(84.92).
Schizandrol A	433.2215 (11.75, 3)	455.2036 (100, 2)	MS^2 $[M+H]^+$: **415.2108(100)***, 400.1865(5.55), 384.1918(42.4); MS^2 $[M+Na]^+$: 409.1609(100).	384.1910(100), 369.1654(25.35), 338.1467(5.85).

[a] differences between the observed and theoretical values; * : the detected DFI.
The fragment ions with high response (intensity >10 000) generated in MS^2 which were shown in bold font and underlined were automatically selected for MS^3 fragmentations.

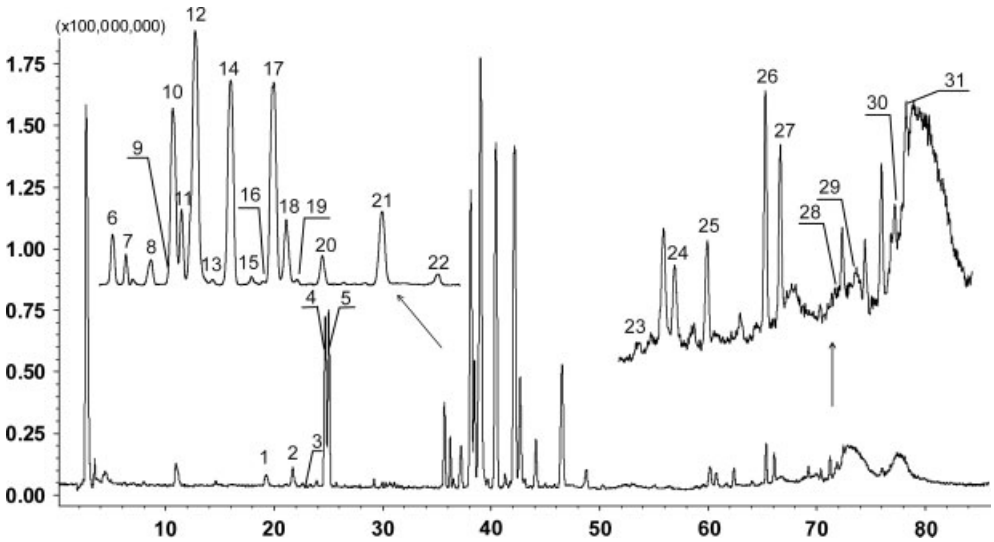

Figure 5. Total ion chromatogram of *Shengmai injection* obtained from the negative ion scan mode.

DFIBES-directed rapid screening and identification

The injection samples were extracted to decrease the interferences from the excipients such as Tween 80. The performance of a variety of organic solvents (ethyl ether, acetic ether, and water-saturated *n*-butanol), singly or in combination, to extract the active constituents from *Shengmai injection*, was investigated. Finally, we chose water-saturated *n*-butanol as the optimized solvents due to its capacity of maximizing the peak areas for the majority of peaks of interest detected.

DFIBES was then used for the rapid screening and identification of ginsenosides and lignans contained in *Shengmai injection*. The DFIs were used as markers for screening and classifying the components detected from *Shengmai injection* into known subfamilies, followed by a 'structure extension' approach based on the serial fragment ions analysis. The mass differences between the observed and theoretical values were tolerated within 20 ppm throughout the whole analysis process. Although the generally accepted TOF/MS accuracy tolerance is within 5 ppm deviation, it might be acceptable[23,34] by setting the mass tolerance at 20 ppm for the complicated matrix analysis, in the view of that TOF/MS accuracies could be severely influenced by the peak interferences. For pure compounds analysis, the mass deviations in our study have been well controlled below 5 ppm (Tables 1 and 2). The MS and MS^n spectra after continuous infusions were almost identical, indicating that the method was highly reproducible.

Detection and identification of ginsenosides in Shengmai injection

Figure 5 showed the TIC of the extract of *Shengmai injection* obtained from the negative ion scan. The DFI corresponding to each kind of ginsenosides were then separately inputted into the workstation to extract the peaks detected from *Shengmai injection*. As a result, peak 7, 11, 12a, 12c, 14b, 14c, 15–18, 20, 21b, 22, and 26–29 were classified as type A ginsenosides;

Journal of MASS SPECTROMETRY

peak 1–6, 8, 9, 12b, 12d, 13, 14a, and 19 were classified as type B ginsenosides; peak 23 and 24 were classified as C or D protopanaxatriol-type ginsenosides; peak 10 was classified as type E ginsenosides (Table 3).

The next step was to elucidate the structures of the ginsenosides using 'structure extension' approach. Here we took peak 12b identification as an example to describe the strategy in detail. According to the fragment behaviors of ginsenosides, sugar units, top-right aliphatic chain, and H_2O were the common chemical groups that were easily lost under CID mode. The mass differences existed between DFI and quasi-molecular ions and other fragment ions were associated with sugar units [e.g. pentose ($C_5H_8O_4$, 132.0422), hexose ($C_6H_{10}O_5$, 162.0528), and deoxyhexose ($C_6H_{10}O_4$, 146.0579)], top-right aliphatic chain (C_6H_{12}, 84.0939), or water (H_2O, 18.0211). For peak 12b, the mass difference between $[aglycone - H]^-$ ion (DFI 1) and quasi-molecular ion (Table 3) was 308.1140, which was assigned to the combined loss of a deoxyhexose and a hexose. The mass difference between the $[aglycone - H]^-$ ion (475.3785) and the fragment ion *m/z* 637.4356 was 162.0571 corresponding to a hexose unit ($C_6H_{10}O_5$), while the fragment ion 146.06 higher than the $[aglycone - H]^-$ ion was absent, indicating that it was a disaccharide rather than two monosaccharides connecting to the aglycone and the hexose was the sugar residue directly attached to the aglycone. The difference between the ion at *m/z* 637.4356 and $[M - H]^-$ ion (783.4925) was 146.0569, indicating the presence of a terminal deoxyhexose unit ($C_6H_{10}O_4$). These fragment ions directly provided detailed structural information about the monosaccharide sequence. Peak 12b was then readily identified to be ginsenoside Rg2.

Using DFIBES, it was even possible to differentiate isomeric saponins with different aglycones. For example, peak 26 and 27 produced almost identical $[M - H]^-$ ions to peak 12b (also peak 13), however, they gave the predominant fragment ions at *m/z* 459.38 and thus were classified into type A ginsenoside. Using the 'Structure extension' approach, peak 26 and 27 were tentatively assigned as a pair of ginsenoside Rg3 epimers. Furthermore, on the basis of the match of retention times, molecular weights and fragmentation patterns with that of the standards, peak 12b and 26 were confirmed as 20(S)-ginsenoside Rg2 and Rg3, respectively, while peak 13 and 27 could then be proposed to be 20(R)-ginsenoside Rg2 and Rg3, respectively.

In summary, 31 peaks attributed to ginsenosides were detected from *Shengmai injection* in a 75-min chromatographic run (Fig. 5). Most of them were rapidly identified using the DFIBES strategy. For the rest components (peak 21a, 24a, 25, 30, and 31) that failed to be identified using DFIBES, we had to make a full fragmentation analysis and comparisons with that from the library, which was actually a difficult task and time consuming. The main cause for the failure was that the corresponding components were characterized with lower concentrations and thus failed to produce the DFIs in the presently used mass conditions. Their tentative identifications were summarized in Table 3.

Detection and identification of lignans in Shengmai injection

The TIC of the extract of *Shengmai injection* obtained from the positive ion scan is shown in Fig. 6. The pseudomolecular ions and their respective major fragment ions were listed in Table 4. The DFI corresponding to each kind of lignans were also separately inputted into the workstation to selecting and classifying the detected peaks. As a result, 18 out of a total 20 peaks detected have been successfully classified into the described lignan subfamilies and thus facilitating the identification process. Only 2 peaks were failed to be classified using DFIBES, because they produced no fragment ions. On the basis of the 'Structure extension' approach, the further identification results are shown in Table 4. In addition, although the isomers could not be distinguished from the mass spectra, we were able to assign the peaks tentatively based on their contents or chromatography behaviors and comparing that with the previously published data. For strict consideration, we listed all possibilities for some peak identifications in Table 4. However, the first one for peak 7, 12, 13, and 15–17 as listed was proposed to be the preferential identification based on the full information analysis. For example, peak 7 was proposed as three possibilities: Schizandrol B, Gomisin O, or Epigomisin O. Xianguo *et al*. reported that *S. chinensis* contained much more Schizandrol B than Gomisin O or Epigomisin O[2,33] and peak 7 detected in the present study gave a relatively strong signal, indicating a high concentration. Therefore, it was more possible for peak 7 to be assigned as Schizandrol B.

Interestingly, no chemical component resourced from *R. ophiopogonis* was detected in either positive or negative ion MS analysis of *Shengmai injection* samples via various extraction methods, which was consistent with the previous results reported by Zhang *et al*.[7] It was unlikely that our method failed to detect such components as ophiopogonin and ophiopogonone contained in *R. ophiopogonis*, because the corresponding authentic standards were readily extracted and detected under this method. Tentatively, it might be concluded that the components in *R. ophiopogonis* were failed to be extracted during the preparation procedures of *Shengmai injection*.

Universal applicability of DFIBES

The presently proposed and developed DFIBES has been proved to be a very practicable and highly efficient method for identifying the complicated components from *Shengmai injection*. Applying this strategy, more than 80% ginsenosides and 90% lignans have been rapidly identified in this study. Due to the great advance on phytochemistry researches, the chemical families (carbon skeleton) of the constituents contained in most known herbal drugs have been generally clarified. Although there are still many components remained unknown, it is now widely acknowledged that most unknown components can be classified into the known chemical families. The chance of discovering a novel carbon skeleton is very low now. Furthermore, there has been accumulated a large set of mass spectra data for the chemical families contained in herbal drugs, which means that the DFI for a certain chemical family can even be theoretically proposed or readily determined from the literature data. Therefore, the presently developed DFIBES would be universally applicable for identifying the components from most herbal drugs and compound prescriptions. Moreover, it is possible for the DFIBES to be extended to the fields of elucidating compounds from other organic matter mixtures such as water quality analysis, natural organic matter analysis in soil, pesticide multiresidue analysis in food, and so on, in the view of that the compounds contained in such matrix can also be classified into families based on the common carbon skeletons.

Table 3. Identification of ginsenosides in *Shengmai injection*

DFI (type)	Peak No.	Rt (min)	PI	MS^n	Identification
Type A	7	36.2	619.3137[B]	945.5376, 783.4874*, 765.4766, 553.2953, 459.3799*.	Ra3/Notoginsenoside R4
	11	38.5	604.3095[B]	945.5409, 783.4918*; MS^3 [945.5452]: 783.4907*, 621.4371, 459.3824*.	Ra1/Ra2/isomer
	12	38.8(a)	619.3158[B]	945.5437, 783.4944*, 765.4721, 459.3863*.	Ra3/Notoginsenoside R4
		39.1(c)	1107.5991[A]	945.5433, 783.4947*, 765.4816, 621.4420, 459.3880*, 375.2929.	Rb1[s]
	14	40.4(b)	604.3095[B]	783.4917*, 765.4785, 621.4320, 538.2884, 459.3869*.	Ra1/Ra2/isomer
		40.5(c)	538.2873[B]	945.5405, 783.4877*, 459.3856*.	Rc[s]
	15	41.3	604.3081[B]	783.4860*, 765.4752, 538.2869.	Ra1/Ra2/isomer
	16	41.7	604.3089[B]	783.4882*.	Ra1/Ra2/isomer
	17	42.2	538.2867[B]	945.5377, 783.4926*, 765.4754, 621.4327, 459.3827*, 375.2878.	Rb2[s]
	18	42.7	1077.5798[A]	783.4885*, 459.3819*, 375.2898; (MS^2 : $[M + 2AcO]^{2-} \rightarrow$)$MS^3$ [538.2869]: 783.4889*.	Rb3[s]
	20	44.1	574.2951[B]	945.5387, 927.5218, 783.4913*, 765.4811, 553.2925.	Ac-Rb1
	21	46.5(b)	945.5402[A]	783.4828*, 621.4359, 537.3397, 459.3825*, 375.2873; MS^3 [783.4860]: 621.4354, 537.3382, 459.3825*, 375.2893.	Rd[s]
	22	48.8	559.2937[B]	783.4945*, 538.2869.	Rs1/Rs2
	26	65.3	783.4915[A]	621.4439, 537.3512, 459.3884*, 375.2915.	20(S)-Rg3[s]
	27	66.1	783.4885[A]	621.4399, 537.3440, 459.3814*, 375.2908.	20(R)-Rg3
	28	69.0	825.4965[A]	783.4851*, 765.4762, 621.4391, 459.3852*.	Rs3/isomer
	29	69.6	825.4991[A]	783.4912*, 621.4381, 459.3799*.	Rs3/isomer
Type B	1	19.3	961.5399[A]	799.4855, 637.4327, 475.3799*.	20-Glc-Rf/isomer
	2	21.7	931.5235[A]	799.4794, 769.4686, 637.4269, 619.4182, 475.3768*, 391.2827*.	Notoginsenoside R1[s]
	3	22.6	961.5395[A]	799.4855, 475.3799*.	20-Glc-Rf/isomer
	4	24.7	799.4821[A]	637.4270, 619.4154, 475.3747*, 391.2831*; (MS^2 : $[M + AcO]^- \rightarrow$)MS^3 [799.4861]: 637.4250, 619.4155, 475.3757*, 391.2819*.	Rg1[s]
	5	25.0	945.5398[A]	799.4772, 783.4825, 765.4717, 637.4258, 619.4166, 601.4140, 475.3747*, 457.3672, 391.2832*, 373.2752; MS^3 [475.3767]: 457.3692*, 391.2834*, 373.2754.	Re[s]
	6	35.7	799.4811[A]	637.4261, 619.4208, 475.3779*, 457.3716, 391.2830*, 373.2719; MS^3 [475.3762]: 457.3716, 391.2837*.	Rf
	8	37.2	769.4738[A]	637.4299, 475.3769*, 457.3661, 391.2859*, 373.2726; MS^3 [475.3794]: 391.2889*.	Notoginsenoside R2/isomer
	9	37.7	769.4738[A]	475.3778*, 391.2851*.	Notoginsenoside R2/isomer
	12	38.9(b)	783.4925[A]	637.4356, 619.4233, 475.3785*, 391.2837*, 373.2780.	20(S)-Rg2[s]
		39.2(d)	637.4316[A]	475.3800*, 391.2867*.	20(S)-Rh1[s]
	13	39.7	783.4895[A]	637.4310, 621.4395, 619.4250, 475.3762*, 391.2839*, 373.2780.	20(R)-Rg2
	14	40.4(a)	637.4306[A]	475.3777*, 391.2833*.	20(R)-Rh1
	19	43.5	697.4557[C]	637.4300, 475.3814*.	F1
C, D type	23	58.9	765.4789[A]	619.4174, 601.4068, 457.3690*.	Rg6/F4
	24	60.8(b)	765.4789[A]	619.4200, 601.4097, 457.3638*.	Rg6/F4
Type E	10	38.1	955.4903[A]	793.4389, 631.3848, 613.3757, 595.3594, 569.3853, 523.3802, 497.3638, 453.3388; MS^3 [793.4339]: 613.3686, 569.3923, 537.3575, 453.3416; MS^3 [613.3702]: 455.3558*, 437.3395, 407.3241; MS^3 [569.3826]: 497.3665, 437.3495; MS^3 [523.3723]: 453.3394.	Ro

Journal of MASS SPECTROMETRY

Table 3. (*Continued*)

DFI (type)	Peak No.	Rt (min)	PI	MS^n	Identification
– [a]	21	46.4(a)	589.3027[D]	–	Rs1/Rs2
	24	60.7(a)	619.4217[A]	–	Rk3/Rh4
	25	62.4	619.4194[A]	–	Rk3/Rh4
	30	71.9	765.4754[A]	603.4286.	Rg5/Rk1
	31	72.5	765.4775[A]	603.4243, 379.1098.	Rg5/Rk1

Types of pseudomolecular ions. A: $[M - H]^-$; B: $[M - 2H]^{2-}$; C: $[M + AcO]^-$; D: $[M - H + AcO]^{2-}$.
[a] : no evident DFI. [s] : constituents with Standards. * : the detected DFI.

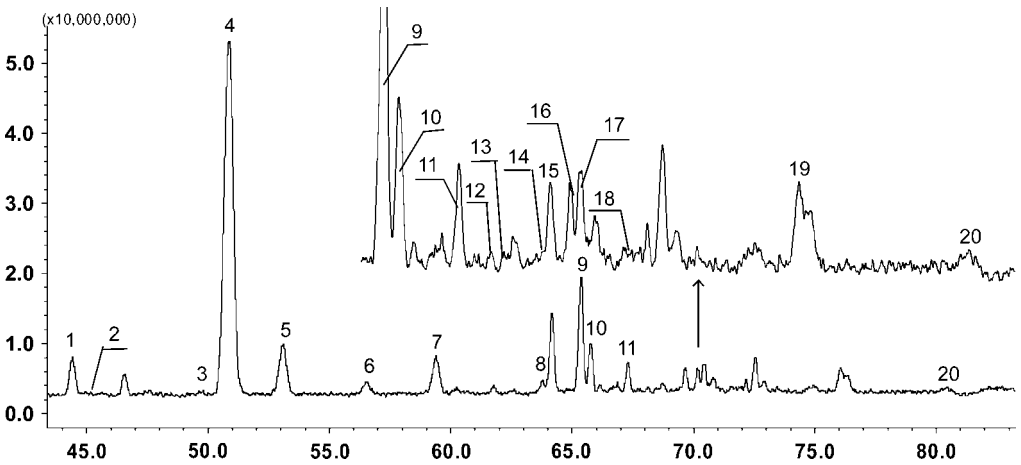

Figure 6. Total ion chromatogram of *Shengmai injection* obtained from the positive ion scan mode.

Restriction of this study and future prospect

In this study, we developed a universal strategy DFIBES for rapid characterization of homologous components in herbal preparation. However, we failed to differentiate some isomers, which were characterized with the same aglycon, sugar units and the same fragmentation behaviors, and with slight differences in the linkage of the sugar moieties, the ring size of the arabinose sugar, or the positions of double bonds in the top-right aliphatic chain. Recently, some approaches[16,17,37,43–45] based on MS techniques to distinguish saponins isomers have been developed and become a fast growing area of interest. For example, Liu *et al*.[37] reported that some cross-ring ions observed in positive mode could provide the linkage information between sugar residues. Song *et al*.[43] differentiated four isomers of steroidal saponins using multiple-stage tandem mass spectrometry combined with electrospray ionization (ESI-MS^n). Therefore, it can be prospectively expected to combine the presently developed DFIBES with other mass-spectrometry-based approaches for more powerful identification of the complicated chemical constituents in herbal drugs and their compound prescriptions in future study.

Theoretically, it is possible that the different families of compounds produced identical fragment ions and thus prone to make wrong classifications by using DFIBES. However, such a phenomenon has not been observed in this study. We consider the case of DFI-based wrong classifications would be very scarce, despite theoretically possible. Even though wrong classifications had been made by DFI approach, it is relatively easy to observe and exclude such a mismatch by the followed fragmentation pathways analysis.

Concluding Remarks

In this work, a modified and universally applicable strategy DFIBES aimed to the rapid identifications of complicated components from TCMP has been successfully developed and validated by taking *Shengmai injection* as an example based on LC-IT-TOF/MS analysis. First, DFI for every chemical family was determined or proposed from fragmentation pattern analysis of the corresponding authentic standards or extract of mono-herb. The 'structure extension' method was then proposed based on the well-demonstrated fragmentation patterns. The presently developed method and strategy were successfully applied into the rapid detection and identification of the complicated components contained in *Shengmai injection*. More than 30 ginsenosides and 20 lignans were readily detected and structurally characterized from *Shengmai injection*. In the view of that the currently known carbon skeletons can cover a large quantity of chemical components contained in most herbal drugs, the presently developed strategy DFIBES would be universally applicable for identifying the complicated components from most herbal drugs and their compound prescriptions.

Acknowledgements

This study was financially supported by National natural science foundation of P.R. China (No. 30572228, 30630076) and the 'eleventh-five years' supporting programs from the Ministry of Science and Technology of P.R. China (2006BAI08B04-05). We thank Professor Longsheng Sheng for his technical assistances.

Table 4. Identification of lignans in *Shengmai injection*

DFI (type)	Peak No.	Rt (min)	PI		MS^n	Identification (1/2/3)
			$[M+H]^+$	$[M+Na]^+$		
Type I	9	65.4	401.1957	423.1805	$MS^2[M+H]^+$: 370.1750, 355.1540; MS^3[370.1751]: 355.1513.	Gomisin N
					$MS^2[M+Na]^+$: 377.1426*	
	14	69.5	403.2135	425.1935	$MS^2[M+H]^+$: 302.1090*, 271.0882.	Schisanhenol/Gomisin K1/Gomisin K2
	18	71.6	403.2124	425.1917	$MS^2[M+H]^+$: 388.1904, 372.1866, 357.1629, 341.1620, 302.1115*, 287.0886, 271.0872; MS^3[372.1855]: 357.1628, 341.1661.	Schisanhenol/Gomisin K1/Gomisin K2
					$MS^2[M+Na]^+$: 379.1525*.	
	19	76.4	417.2283	439.2110	$MS^2[M+H]^+$: 402.2029, 386.2104, 371.1830, 347.1451, 332.1250, 316.1292*, 301.1068, 285.1106.	Schizandrin A^s
Type II	1	44.4	433.2203	455.2036	$MS^2[M+H]^+$: 415.2111*, 400.1900, 384.2001; $MS^2[M+Na]^+$: 409.1565.	Gomisin S
	2	45.0	419.2084	441.1903	$MS^2[M+H]^+$: 401.1952*, 370.1771.	Gomisin H/Gomisin T
	3	49.8	433.2225	455.2041	$MS^2[M+H]^+$: 415.2206*.	Isoschizandrin
	4	50.9	433.2236	455.2033	$MS^2[M+H]^+$: 415.2123*, 400.1877, 384.1929; $MS^2[M+Na]^+$: 409.1562.	Schizandrol A^s
	7	59.4	417.1928	439.1723	$MS^2[M+H]^+$: 399.1769*.	Schizandrol B/Gomisin O/Epigomisin O
Type III	8	63.8	501.2471	523.2285	$MS^2[M+H]^+$: 401.2007*.	Tigloyl gomisin H/Angeloyl gomisin H
	10	65.8(b)	501.2490	523.2297	$MS^2[M+H]^+$: 483.2437, 401.2026*.	Tigloyl gomisin H/Angeloyl gomisin H
Type IV	10	65.7(a)	–	553.2399	$MS^2[M+Na]^+$: 453.1792*, 356.1598, 341.1305, 325.095.	Tigloyl gomisin Q/Angeloyl gomisin Q
	11	67.3	–	553.2413	$MS^2[M+Na]^+$: 453.1865*, 387.1805, 372.1606, 356.1572.	Tigloyl gomisin Q/Angeloyl gomisin Q
	12	68.1	–	559.1922	$MS^2[M+Na]^+$: 437.1498*, 371.1404, 356.1228, 340.1309.	Gomisin G/Schisantherin A
	13	68.4	–	537.2098	$MS^2[M+Na]^+$: 437.1594*.	Gomisin F/Schisantherin B/Schisantherin C
	15	69.7	–	537.2097	$MS^2[M+Na]^+$: 437.1673*, 340.1186.	Schisantherin B/Schisantherin C/Gomisin F
	16	70.2	537.2138	559.1943	$MS^2[M+Na]^+$: 437.1573*, 371.1488, 356.1281, 340.1310, 325.1104.	Schisantherin A/Gomisin G
	17	70.5	–	537.2077	$MS^2[M+Na]^+$: 437.1584*, 340.1329.	Schisantherin C/Schisantherin B/Gomisin F
Type V	6	56.5	531.2206	553.2033	$MS^2[M+Na]^+$: 507.1996*, 391.1119.	Gomisin D
– [a]	5	53.1	387.1795	409.1610	–	Gomisin M1/Gomisin M2/Gomisin L1/Gomisin L2
	20	80.4	401.1953	423.1779	–	Schizandrin B^s

[a]: no evident DFI. ^{s}: constituents with standards. *: the detected DFI.

References

[1] Y. Liu, J. Yang, Z. Cai. Chemical investigation on Sijunzi decoction and its two major herbs Panax ginseng and Glycyrrhiza uralensis by LC/MS/MS. *Journal of Pharmaceutical and Biomedical Analysis* **2006**, *41*, 1642.

[2] X. G. He, L. Z. Lian, L. Z. Lin. Analysis of lignan constituents from Schisandra chinensis by liquid chromatography-electrospray mass spectrometry. *Journal of Chromatography A* **1997**, *757*, 81.

[3] L. Z. Lin, X. G. He, L. Z. Lian, W. King, J. Elliott. Liquid chromatographic-electrospray mass spectrometric study of the phthalides of Angelica sinensis and chemical changes of Z-ligustilide. *Journal of Chromatography A* **1998**, *810*, 71.

[4] H. Zhang, P. Shen, Y. Cheng. Identification and determination of the major constituents in traditional chinese medicine Si-Wu-Tang by HPLC coupled with DAD and ESI-MS. *Journal of Pharmaceutical and Biomedical Analysis* **2004**, *34*, 705.

[5] N. Fuzzati, B. Gabetta, K. Jayakar, R. Pace, F. Peterlongo. Liquid chromatography-electrospray mass spectrometric identification of ginsenosides in Panax ginseng roots. *Journal of Chromatography A* **1999**, *854*, 69.

[6] Q. Tian, S. J. Schwartz. Mass spectrometry and tandem mass spectrometry of citrus limonoids. *Analytical Chemistry* **2003**, *75*, 5451.

[7] H. J. Zhang, Y. J. Wu, Y. Y. Cheng. Analysis of 'SHENMAI' injection by HPLC/MS/MS. *Journal of Pharmaceutical and Biomedical Analysis* **2003**, *31*, 175.
[8] I. Parejo, O. Jauregui, F. Viladomat, J. Bastida, C. Codina. Characterization of acylated flavonoid-O-glycosides and methoxylated flavonoids from Tagetes maxima by liquid chromatography coupled to electrospray ionization tandem mass spectrometry. *Rapid Communications in Mass Spectrometry* **2004**, *18*, 2801.
[9] Y. Sun, W. Li, J. F. Fitzloff, R. B. van Breemen. Liquid chromatography/electrospray tandem mass spectrometry of terpenoid lactones in Ginkgo biloba. *Journal of Mass Spectrometry* **2005**, *40*, 373.
[10] D. C. van Setten, G. J. ten Hove, E. J. Wiertz, J. P. Kamerling, G. van de Werken. Multiple-stage tandem mass spectrometry for structural characterization of saponins. *Analytical Chemistry* **1998**, *70*, 4401.
[11] X. Huang, F. Song, Z. Liu, S. Liu. Studies on lignan constituents from Schisandra chinensis (Turcz.) Baill. fruits using high-performance liquid chromatography/electrospray ionization multiple-stage tandem mass spectrometry. *Journal of Mass Spectrometry* **2007**, *42*, 1148.
[12] A. H. Liu, H. Guo, M. Ye, Y. H. Lin, J. H. Sun, M. Xu, D. A. Guo. Detection, characterization and identification of phenolic acids in Danshen using high-performance liquid chromatography with diode array detection and electrospray ionization mass spectrometry. *Journal of Chromatography A* **2007**, *1161*, 170.
[13] J. Liu, X. Yang, J. He, M. Xia, L. Xu, S. Yang. Structure analysis of triterpene saponins in Polygala tenuifolia by electrospray ionization ion trap multiple-stage mass spectrometry. *Journal of Mass Spectrometry* **2007**, *42*, 861.
[14] F. Sun, Q. He, P. Shi, P. Xiao, Y. Cheng. Characterization and identification of triterpenoid saponins in crude extracts from Clematis spp. by high-performance liquid chromatography/electrospray ionization with multi-stage tandem mass spectrometry. *Rapid Communications in Mass Spectrometry* **2007**, *21*, 3743.
[15] P. C. Eklund, M. J. Backman, L. A. Kronberg, A. I. Smeds, R. E. Sjoholm. Identification of lignans by liquid chromatography-electrospray ionization ion-trap mass spectrometry. *Journal of Mass Spectrometry* **2008**, *43*, 97.
[16] B. Li, Z. Abliz, G. Fu, M. Tang, S. Yu. Characteristic fragmentation behavior of some glucuronide-type triterpenoid saponins using electrospray ionization tandem mass spectrometry. *Rapid Communications in Mass Spectrometry* **2005**, *19*, 381.
[17] B. Li, Z. Abliz, M. Tang, G. Fu, S. Yu. Rapid structural characterization of triterpenoid saponins in crude extract from Symplocos chinensis using liquid chromatography combined with electrospray ionization tandem mass spectrometry. *Journal of Chromatography A* **2006**, *1101*, 53.
[18] A. Tolonen, J. Uusitalo. Fast screening method for the analysis of total flavonoid content in plants and foodstuffs by high-performance liquid chromatography/electrospray ionization time-of-flight mass spectrometry with polarity switching. *Rapid Communications in Mass Spectrometry* **2004**, *18*, 3113.
[19] E. C. Chan, S. L. Yap, A. J. Lau, P. C. Leow, D. F. Toh, H. L. Koh. Ultra-performance liquid chromatography/time-of-flight mass spectrometry based metabolomics of raw and steamed Panax notoginseng. *Rapid Communications in Mass Spectrometry* **2007**, *21*, 519.
[20] Z. Zhu, H. Zhang, L. Zhao, X. Dong, X. Li, Y. Chai, G. Zhang. Rapid separation and identification of phenolic and diterpenoid constituents from Radix Salvia miltiorrhizae by high-performance liquid chromatography diode-array detection, electrospray ionization time-of-flight mass spectrometry and electrospray ionization quadrupole ion trap mass spectrometry. *Rapid Communications in Mass Spectrometry* **2007**, *21*, 1855.
[21] L. Zhao, Z. Y. Lou, Z. Y. Zhu, G. Q. Zhang, Y. F. Chai. Characterization of constituents in Stellera chamaejasme L. by rapid-resolution liquid chromatography-diode array detection and electrospray ionization time-of-flight mass spectrometry. *Biomedical Chromatography* **2008**, *22*, 64.
[22] R. Li, Y. Zhou, Z. Wu, L. Ding. ESI-QqTOF-MS/MS and APCI-IT-MS/MS analysis of steroid saponins from the rhizomes of Dioscorea panthaica. *Journal of Mass Spectrometry* **2006**, *41*, 1.
[23] C. M. Li, X. L. Zhang, X. Y. Xue, F. F. Zhang, Q. Xu, X. M. Liang. Structural characterization of iridoid glucosides by ultra-performance liquid chromatography/electrospray ionization quadrupole time-of-flight tandem mass spectrometry. *Rapid Communications in Mass Spectrometry* **2008**, *22*, 1941.
[24] Y. Wang, X. Lu, G. Xu. Development of a comprehensive two-dimensional hydrophilic interaction chromatography/quadrupole time-of-flight mass spectrometry system and its application in separation and identification of saponins from Quillaja saponaria. *Journal of Chromatography A* **2008**, *1181*, 51.
[25] J. Qu, Q. Liang, G. Luo, Y. Wang. Screening and identification of glycosides in biological samples using energy-gradient neutral loss scan and liquid chromatography tandem mass spectrometry. *Analytical Chemistry* **2004**, *76*, 2239.
[26] J. S. You, H. F. Huang, Y. L. Chang, Y. S. Lee. Sheng-mai-san reduces adriamycin-induced cardiomyopathy in rats. *The American Journal of Chinese Medicine* **2006**, *34*, 295.
[27] K. Yu, Y. Ma, Q. Shao, H. Qu, Y. Cheng. Simultaneously determination of five ginsenosides in rabbit plasma using solid-phase extraction and HPLC/MS technique after intravenous administration of 'SHENMAI' injection. *Journal of Pharmaceutical and Biomedical Analysis* **2007**, *44*, 532.
[28] N. Fuzzati. Analysis methods of ginsenosides. *Journal of Chromatography. B, Analytical Technologies in the Biomedical and Life Sciences* **2004**, *812*, 119.
[29] H. F. Dai, W. L. Mei. Ophiopojaponin D, a new phenylpropanoid glycoside from Ophiopogon japonicus Ker-Gawl. *Archives of Pharmacal Research* **2005**, *28*, 1236.
[30] Z. H. Cheng, T. Wu, B. Y. Yu. Steroidal glycosides from tubers of Ophiopogon japonicus. *Journal of Asian Natural Products Research* **2006**, *8*, 555.
[31] J. M. Chang, C. C. Shen, Y. L. Huang, M. Y. Chien, J. C. Ou, B. J. Shieh, C. C. Chen. Five new homoisoflavonoids from the tuber of Ophiopogon japonicus. *Journal of Natural Products* **2002**, *65*, 1731.
[32] M. Ye, D. Guo, G. Ye, C. Huang. Analysis of homoisoflavonoids in Ophiopogon japonicus by HPLC-DAD-ESI-MSn. *Journal of the American Society for Mass Spectrometry* **2005**, *16*, 234.
[33] L. Opletal, H. Sovova, M. Bartlova. Dibenzo[a,c]cyclooctadiene lignans of the genus Schisandra: importance, isolation and determination. *Journal of Chromatography. B, Analytical Technologies in the Biomedical and Life Sciences* **2004**, *812*, 357.
[34] J. Sultan, W. Gabryelski. Structural identification of highly polar nontarget contaminants in drinking water by ESI-FAIMS-Q-TOF-MS. *Analytical Chemistry* **2006**, *78*, 2905.
[35] E. B. Kujawinski, M. D. Behn. Automated analysis of electrospray ionization fourier transform ion cyclotron resonance mass spectra of natural organic matter. *Analytical Chemistry* **2006** ***78***, 4363.
[36] X. S. Miao, C. D. Metcalfe, C. Hao, R. E. March. Electrospray ionization mass spectrometry of ginsenosides. *Journal of Mass Spectrometry* **2002**, *37*, 495.
[37] S. Liu, M. Cui, Z. Liu, F. Song, W. Mo. Structural analysis of saponins from medicinal herbs using electrospray ionization tandem mass spectrometry. *Journal of the American Society for Mass Spectrometry* **2004**, *15*, 133.
[38] B. Domon, C. E. Costello. A systematic nomenclature for carbohydrate fragmentations in FAB-MS/MS spectra of glycoconjugates. *Glycoconjugate Journal* **1988**, *5*, 397.
[39] K. Zou, S. Zhu, C. Tohda, S. Cai, K. Komatsu. Dammarane-type triterpene saponins from Panax japonicus. *Journal of Natural Products* **2002**, *65*, 346.
[40] X. Huang, F. Song, Z. Liu, S. Liu. Structural characterization and identification of dibenzocyclooctadiene lignans in Fructus Schisandrae using electrospray ionization ion trap multiple-stage tandem mass spectrometry and electrospray ionization Fourier transform ion cyclotron resonance multiple-stage tandem mass spectrometry. *Analytica Chimica Acta* **2008**, *615*, 124.
[41] H. B. Zhai, P. Z. Cong. Mass spectrometric studies on dibenocyclooctadiene lignan compounds from schisandraceae plants. *Acta Pharmacologica Sinica* **1990**, *25*, 110.
[42] M. Ye, Y. Yan, D. A. Guo. Characterization of phenolic compounds in the Chinese herbal drug Tu-Si-Zi by liquid chromatography coupled to electrospray ionization mass spectrometry. *Rapid Communications in Mass Spectrometry* **2005**, *19*, 1469.
[43] F. Song, M. Cui, Z. Liu, B. Yu, S. Liu. Multiple-stage tandem mass spectrometry for differentiation of isomeric saponins. *Rapid Communications in Mass Spectrometry* **2004**, *18*, 2241.

[44] T. W. Chan, P. P. But, S. W. Cheng, I. M. Kwok, F. W. Lau, H. X. Xu. Differentiation and authentication of Panax ginseng, Panax quinquefolius, and ginseng products by using HPLC/MS. *Analytical Chemistry* **2000**, *72*, 1281.

[45] Y. Bao, C. Li, H. Shen, F. Nan. Determination of saikosaponin derivatives in Radix bupleuri and in pharmaceuticals of the chinese multiherb remedy xiaochaihu-tang using liquid chromatographic tandem mass spectrometry. *Analytical Chemistry* **2004**, *76*, 4208.